Title

Cooperation of the Ebola Virus Proteins VP40 and GP1,2 with BST2 To Activate NF-κB Independently of Virus-Like Particle Trapping

Journal

Journal of Virology, 91(22)

ISSN

0022-538X

Authors

Rizk, Maryan G

Basler, Christopher F

Guatelli, John

Publication Date

2017-11-15

DOI

10.1128/jvi.01308-17

Peer reviewed

AMERICAN SOCIETY FOR MICROBIOLOGY | Journal of Virology®

VIRUS-CELL INTERACTIONS

Cooperation of the Ebola Virus Proteins VP40 and $GP_{1,2}$ with BST2 To Activate NF-κB Independently of Virus-Like Particle Trapping

Maryan G. Rizk,[a] Christopher F. Basler,[b] John Guatelli[a,c]

University of California San Diego, La Jolla, California, USA[a]; Center for Microbial Pathogenesis, Institute for Biomedical Sciences, Georgia State University, Atlanta, Georgia, USA[b]; Veterans Affairs San Diego Healthcare System, San Diego, California, USA[c]

ABSTRACT BST2 is a host protein with dual functions in response to viral infections: it traps newly assembled enveloped virions at the plasma membrane in infected cells, and it induces NF-κB activity, especially in the context of retroviral assembly. In this study, we examined whether Ebola virus proteins affect BST2-mediated induction of NF-κB. We found that the Ebola virus matrix protein, VP40, and envelope glycoprotein, GP, each cooperate with BST2 to induce NF-κB activity, with maximal activity when all three proteins are expressed. Unlike human immunodeficiency virus type 1 Vpu protein, which antagonizes both virion entrapment and the activation of NF-κB by BST2, Ebola virus GP does not inhibit NF-κB signaling even while it antagonizes the entrapment of virus-like particles. GP from Reston ebolavirus, a nonpathogenic species in humans, showed a phenotype similar to that of GP from Zaire ebolavirus, a highly pathogenic species, in terms of both the activation of NF-κB and the antagonism of virion entrapment. Although Ebola virus VP40 and GP both activate NF-κB independently of BST2, VP40 is the more potent activator. Activation of NF-κB by the Ebola virus proteins either alone or together with BST2 requires the canonical NF-κB signaling pathway. Mechanistically, the maximal NF-κB activation by GP, VP40, and BST2 together requires the ectodomain cysteines needed for BST2 dimerization, the putative BST2 tetramerization residue L70, and Y6 of a potential hemi-ITAM motif in BST2's cytoplasmic domain. BST2 with a glycosylphosphatidylinositol (GPI) anchor signal deletion, which is not expressed at the plasma membrane and is unable to entrap virions, activated NF-κB in concert with the Ebola virus proteins at least as effectively as wild-type BST2. Signaling by the GPI anchor mutant also depended on Y6 of BST2. Overall, our data show that activation of NF-κB by BST2 is independent of virion entrapment in the case of Ebola virus. Nonetheless, BST2 may induce or amplify proinflammatory signaling during Ebola virus infection, potentially contributing to the dysregulated cytokine response that is a hallmark of Ebola virus disease.

IMPORTANCE Understanding how the host responds to viral infections informs the development of therapeutics and vaccines. We asked how proinflammatory signaling by the host protein BST2/tetherin, which is mediated by the transcription factor NF-κB, responds to Ebola virus proteins. Although the Ebola virus envelope glycoprotein ($GP_{1,2}$) antagonizes the trapping of newly formed virions at the plasma membrane by BST2, we found that it does not inhibit BST2's ability to induce NF-κB activity. This distinguishes $GP_{1,2}$ from the HIV-1 protein Vpu, the prototype BST2 antagonist, which inhibits both virion entrapment and the induction of NF-κB activity. Ebola virus $GP_{1,2}$, the Ebola virus matrix protein VP40, and BST2 are at least additive with respect to the induction of NF-κB activity. The effects of these proteins converge on an intracellular signaling pathway that depends on a protein modification termed

Received 1 August 2017 **Accepted** 28 August 2017

Accepted manuscript posted online 6 September 2017

Citation Rizk MG, Basler CF, Guatelli J. 2017. Cooperation of the Ebola virus proteins VP40 and $GP_{1,2}$ with BST2 to activate NF-κB independently of virus-like particle trapping. J Virol 91:e01308-17. https://doi.org/10.1128/JVI.01308-17.

Editor Wesley I. Sundquist, University of Utah

Address correspondence to John Guatelli, jguatelli@ucsd.edu.

neddylation. Better mechanistic understanding of these phenomena could provide targets for therapies that modulate the inflammatory response during Ebola virus disease.

KEYWORDS BST2, Ebola virus, NF-κB, VP40

BST2 (bone marrow stromal cell antigen 2), also known as tetherin, is an interferon-inducible antiviral protein (1–3). Two functions of BST2 have been associated with viral infections: BST2 traps newly assembled enveloped virions at the plasma membrane (PM) in infected cells, and it induces the activation of the proinflammatory transcription factor NF-κB (2–5). The exact mechanism by which BST2 initiates NF-κB activity in response to viral infections is unknown. One model suggests that upon trapping of virions at the plasma membrane, aggregation of BST2 initiates a kinase cascade culminating in the activation of NF-κB and the release of proinflammatory cytokines (4). This model is based on signaling studies that used retroviruses, namely, murine leukemia virus (MLV) and human immunodeficiency virus type 1 (HIV-1), lacking the accessory protein Vpu, which enhances virion release by antagonizing BST2 (4). Another model suggests that BST2-mediated activation of NF-κB is independent of virion entrapment; this model is based on the identification of a BST2 mutant that is unable to entrap virions but retains signaling activity, as discussed below (5). Since BST2's restrictive function is not unique to retroviruses, studies using other families of enveloped viruses have the potential to extend or challenge the above-mentioned models of the BST2 signaling mechanism and characterize how BST2 responds to the expression of viral genes.

BST2 is a dimeric type II transmembrane (TM) protein that physically tethers nascent virions of enveloped viruses to the plasma membrane in infected cells (6). BST2 contains an N-terminal cytoplasmic tail, a transmembrane domain, a rigid coiled-coil ectodomain, and a glycosylphosphatidylinositol (GPI) anchor at its C terminus (7). This unusual, if not unique, structure enables BST2 to trap newly formed virions on the cell surface by physically cross-linking the lipid bilayers of the plasma membrane and the enveloped virion (8). BST2 requires a tyrosine residue (Y6) within its cytoplasmic tail to activate NF-κB, but not to entrap virions (4, 5, 9). The GPI anchor of BST2 is required for virion entrapment, while it is dispensable for NF-κB activation in some studies but required in others (4, 5, 9). These findings suggest that virion entrapment, while apparently contributory to BST2-mediated activation of NF-κB by retroviruses, might be generally unnecessary for BST2 to induce NF-κB activity. Consensus in the field exists regarding the notion that BST2 signals through a transforming growth factor β (TGF-β)-activated kinase 1 (TAK1)-dependent cascade leading to the activation of the canonical NF-κB pathway (4, 5). This pathway requires the degradation of IκB by a cullin-1-based ubiquitin ligase complex, which requires modification of cullin-1 with the ubiquitin-like molecule nedd8 (5, 10, 11).

Various viral proteins have evolved to counteract the BST2 function of virion entrapment (12–15). As mentioned above, HIV-1 Vpu is the prototype antagonist of BST2 (2, 3); Vpu mistraffics BST2 away from the plasma membrane, removes it from virion assembly sites, and targets it for degradation (13, 16–21). On the other hand, the Ebola virus envelope glycoprotein ($GP_{1,2}$) antagonizes BST2 to enhance virion release through an unclear mechanism that requires neither the removal of BST2 from the cell surface nor its degradation but might instead involve dissociation of BST2 from the Ebola virus matrix protein, VP40; this activity requires proper N-linked glycosylation of the GP1 subunit and the interaction of BST2 with the GP2 subunit (12, 22–28).

In this study, we used Ebola virus $GP_{1,2}$ as a tool to determine whether, within the context of a filovirus, the antagonism of virion entrapment impairs the ability of BST2 to induce NF-κB activity. To do this, we used an Ebola virus-like particle (VLP) model using the matrix protein, VP40. VP40 expression is sufficient to produce particles that resemble actual virions of Ebola virus and incorporate $GP_{1,2}$ (29). $GP_{1,2}$ is a glycoprotein that forms trimeric surface spikes on the Ebola virions and VLPs (29, 30). $GP_{1,2}$ is a

heterodimer that consists of GP1 and GP2, which are linked by disulfide bonds; GP2 contains the transmembrane domain of $GP_{1,2}$ (31). We found that, unlike Vpu, $GP_{1,2}$ did not inhibit NF-κB signaling despite antagonizing BST2-mediated VLP entrapment. Rather, $GP_{1,2}$ cooperated with BST2 and VP40 to produce maximal NF-κB activity compared to BST2 signaling in response to VP40 expression alone. To further support the independence of virion entrapment and NF-κB activation by BST2, we found that BST2 lacking its GPI anchor signal (ΔGPI BST2), which is not expressed at the cell surface and is defective for virion entrapment (5), was fully functional for NF-κB activation, both alone and in the context of expression of Ebola virus $GP_{1,2}$ and VP40. Thus, our data indicate that virion entrapment is not required for BST2 to induce NF-κB activity in the case of Ebola virus and that relief of virion entrapment by Ebola virus $GP_{1,2}$ does not inhibit NF-κB activity. The data nonetheless leave open the possibility that BST2 acts as an amplifier of the signal generated by the Ebola virus proteins.

RESULTS

Ebola virus $GP_{1,2}$ does not inhibit BST2-mediated activation of NF-κB. Since Ebola virus $GP_{1,2}$ is an antagonist of virion entrapment, like HIV-1 Vpu, we hypothesized that it could decrease BST2 signaling as a result of decreased virion entrapment. To test this hypothesis, we used Ebola virus VP40 as a model for VLP formation and release and an NF-κB-responsive luciferase reporter assay. We analyzed three independent experiments, each containing four replicates for the groups compared (Fig. 1 and Tables 1 and 2). In these experiments, we used HEK293T cells engineered to express BST2 stably and compared them to parental cells. Stable expression of BST2 in HEK293T cells (designated Hu6) induced a significant, although quantitatively small, increase of NF-κB activity compared to the background activity in parental HEK293T cells, which express undetectable levels of BST2 as measured by Western blotting (WB) and flow cytometry (Fig. 1A and B and Tables 1 and 2; see Fig. 7B). We found that $GP_{1,2}$ expressed in BST2 stable cells (Hu6) significantly increased NF-κB activity compared to Hu6 cells alone or to $GP_{1,2}$ expressed in parental 293T cells (Tables 1 and 2). In contrast, Vpu expressed in Hu6 cells significantly decreased NF-κB activity compared to Hu6 cells alone but not compared to Vpu expression in parental 293T cells. Expression of $GP_{1,2}$ significantly increased the NF-κB activity of Hu6 (BST2-expressing) cells expressing VP40, while Vpu significantly decreased this activity (Fig. 1A and Tables 1 and 2); these data indicate that, unlike Vpu, Ebola virus $GP_{1,2}$ is not an antagonist of signaling. Interestingly, we found that VP40 and $GP_{1,2}$ induced NF-κB activity regardless of BST2 expression, although a trend of increased NF-κB activity in Hu6 cells compared to parental 293T cells was apparent (Fig. 1A and Table 2), suggesting dependence on BST2 expression for the highest signal. The Western blot in Fig. 1B confirmed the expression of the various proteins in a representative experiment. Notably, the expression of VP40 was slightly greater in Hu6 than in parental 293T cells (Fig. 1B, compare lane 2 with 8 and 6 with 12).

We next determined whether the trends observed for NF-κB activation by BST2 and the Ebola virus proteins were recapitulated in cells transiently expressing BST2, because we wanted to test various mutants of BST2 for mechanistic studies, as shown below. To do this, we transfected parental HEK293T cells to transiently express BST2 either alone or with the viral proteins and the reporter plasmids and measured NF-κB activity (Fig. 2A and Table 3). When we analyzed two sets of experiments, each containing four replicates, we found that transient expression of BST2 induced a significant increase in NF-κB activity compared to the background empty vector (pcDNA) control. We found that $GP_{1,2}$ coexpressed with BST2 did not decrease NF-κB activity compared to BST2 alone, whereas Vpu did (Tables 3 and 4). Expression of $GP_{1,2}$ significantly increased NF-κβ activity in concert with BST2 and VP40, while Vpu significantly decreased this activity (Tables 3 and 4). Thus, the overall effects of $GP_{1,2}$ and Vpu on BST2-mediated NF-κB signaling were similar in BST2 stable cells and cells transiently expressing BST2. However, we observed differences in protein expression between the two systems using Western blotting (Fig. 1B and 2B). Levels of transiently expressed BST2 were

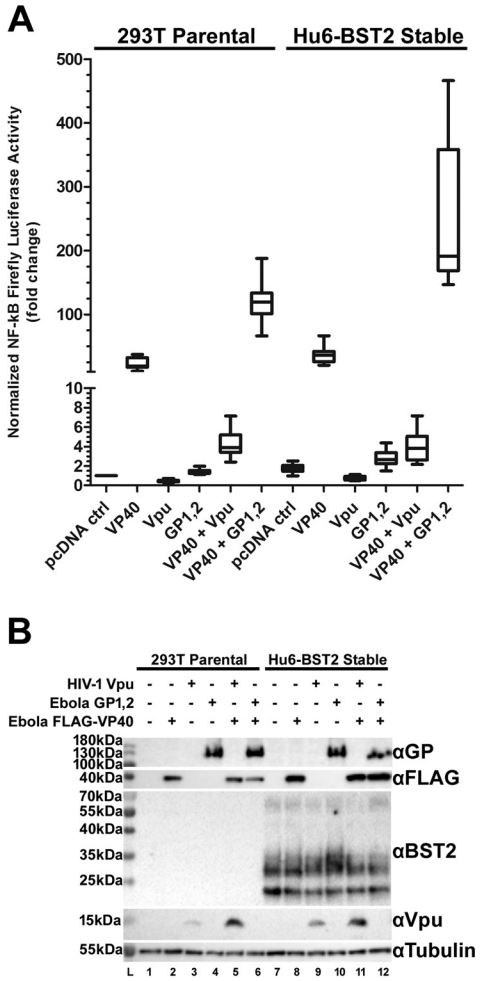

FIG 1 Ebola virus $GP_{1,2}$ and VP40 cooperate with BST2 to induce NF-κB activity in Hu6 cells. (A) Hu6 cells (HEK293T cells stably engineered to express BST2 WT) or parental 293T cells were transfected with 75 ng of a plasmid expressing *Renilla* luciferase (to measure transfection efficiency) and 150 ng of a plasmid expressing firefly luciferase downstream of NF-κB response sequences (to measure NF-κB activity). Wherever indicated on the graph, cells were transfected with the following quantities of plasmids: 900 ng VP40, 900 ng $GP_{1,2}$, and/or 900 ng Vpu. An empty vector, pcDNA3.1, was used to equalize the total amount of plasmids transfected in each sample. After 24 h, firefly luciferase and *Renilla* luciferase activities were measured by luminometry. The ratio of firefly to *Renilla* luciferase luminescence for each condition is graphed relative to parental HEK293T cells transfected only with the pcDNA plasmid, which was set at 1.0; this value represents the fold enhancement of NF-κB activity by the tested proteins. The boxes represent medians within the 25th to 75th percentile range of data, and the whiskers represent maximum and minimums. Statistical analyses and values are presented in Tables 1 and 2. (B) Western blots of total cell lysates from one representative experiment out of three. Ebola virus GP, HIV-1 Vpu, and BST2 were detected using their respective rabbit antisera. VP40 was detected using mouse anti-FLAG antibody. Tubulin was used as a loading control and detected using mouse anti-tubulin antibody.

increased due to the expression of the Ebola viral proteins (Fig. 2B, lane 4 versus 6, 10, and 12); this effect was not observed in the stable Hu6 cells, where the expression of Ebola virus proteins did not increase BST2 expression (Fig. 1B, lane 7 versus 8, 10, and 12). Finally, we wanted to confirm the ability of $GP_{1,2}$ and Vpu to antagonize the virion-trapping function of BST2. As expected, we found that both $GP_{1,2}$ and Vpu antagonized BST2-mediated entrapment and restored VLP release (Fig. 2B, lanes 7 to 12 for VLPs). Overall, these data indicated that Ebola virus $GP_{1,2}$ does not inhibit BST2 signaling despite enhancing virion release; this result does not support our initial hypothesis and suggests instead a disconnect between virion entrapment and NF-κB activation.

$GP_{1,2}$s from the Zaire and Reston ebolavirus species cooperate similarly with VP40 and BST2 to activate NF-κB. We wanted to determine whether $GP_{1,2}$s from Zaire

TABLE 1 Statistical analysis of NF-κB luciferase signaling data presented in Fig. 1A[a]

Group 1	Group 2	Wilcoxon rank sum	Kruskal-Wallis (control = 1)	Dunn's	Significant
pcDNA[b]	VP40	<0.0001[f]			Yes
	Vpu	<0.0001[f]			Yes
	$GP_{1,2}$	0.0002[e]			Yes
	Hu6 + pcDNA	<0.0001[f]			Yes
VP40 + Vpu	VP40		<0.0001[f]	[c]	Yes
	Vpu			[c]	Yes
VP40 + $GP_{1,2}$	VP40		<0.0001[f]	[c]	Yes
	$GP_{1,2}$			[e]	Yes
Hu6 + VP40	VP40		<0.0001[f]	[g]	No
	Hu6 + pcDNA			[e]	Yes
Hu6 + Vpu	Vpu		<0.0001[f]	[g]	No
	Hu6			[d]	Yes
Hu6 + $GP_{1,2}$	$GP_{1,2}$		<0.0001[f]	[e]	Yes
	Hu6 + pcDNA			[c]	Yes
Hu6 + VP40 + Vpu	Hu6 + Vpu		<0.0001[f]	[d]	Yes
	Hu6 + VP40			[d]	Yes
	VP40 + Vpu			[g]	No
Hu6 + VP40 + $GP_{1,2}$	Hu6 + $GP_{1,2}$		<0.0001[f]	[e]	Yes
	Hu6 + VP40			[e]	Yes
	VP40 + $GP_{1,2}$			[g]	No

[a]The indicated viral proteins were expressed in parental HEK293T cells except where indicated by "Hu6," which indicates the use of HEK293T cells constitutively expressing BST2.
[b]A plasmid expressing no viral protein used as a negative control.
[c]$P \leq 0.05$.
[d]$P \leq 0.005$.
[e]$P \leq 0.0005$.
[f]$P < 0.0001$.
[g]Not significant.

and Reston ebolavirus species differed in their abilities to activate NF-κB in concert with BST2 or to counteract BST2-mediated VLP entrapment, because Reston ebolavirus is not pathogenic in humans while Zaire ebolavirus is highly pathogenic. To address this question, we tested two clones of Zaire ebolavirus $GP_{1,2}$ (1976 Zaire ebolavirus $GP_{1,2}$ [76 $zGP_{1,2}$] and 2014 Zaire ebolavirus $GP_{1,2}$ [14 $zGP_{1,2}$]) and Reston ebolavirus $GP_{1,2}$ ($rGP_{1,2}$) in an experiment similar in setup to that presented in Fig. 2. The 1976 Zaire ebolavirus

TABLE 2 Normalized NF-κB luciferase values presented in Fig. 1A[a]

Group	Median[c]	Min[d]	Max[e]	25th percentile	75th percentile
VP40	18.92	10.99	37.27	17.30	32.35
Vpu	0.46	0.30	0.72	0.37	0.52
$GP_{1,2}$	1.42	1.13	1.98	1.24	1.54
Hu6-pcDNA[b]	1.81	0.98	2.53	1.46	2.05
VP40 + Vpu	3.88	2.41	7.14	3.43	5.19
VP40 + $GP_{1,2}$	119.30	66.22	187.70	101.10	133.50
Hu6 + VP40	36.50	20.27	66.63	25.72	42.13
Hu6 + Vpu	0.6977	0.4908	1.107	0.5449	0.9299
Hu6 + $GP_{1,2}$	2.68	1.49	4.37	2.25	3.37
Hu6 + VP40 + Vpu	3.80	2.17	7.16	2.63	5.05
Hu6 + VP40 + $GP_{1,2}$	191.50	146.70	466.20	168.70	358.40

[a]The indicated viral proteins were expressed in parental HEK293T cells except where indicated by "Hu6," which indicates the use of HEK293T cells constitutively expressing BST2.
[b]A plasmid control expressing no viral protein. The value for pcDNA in parental HEK293T cells was arbitrarily set to 1.0.
[c]Control = 1.
[d]Min, minimum value.
[e]Max, maximum value.

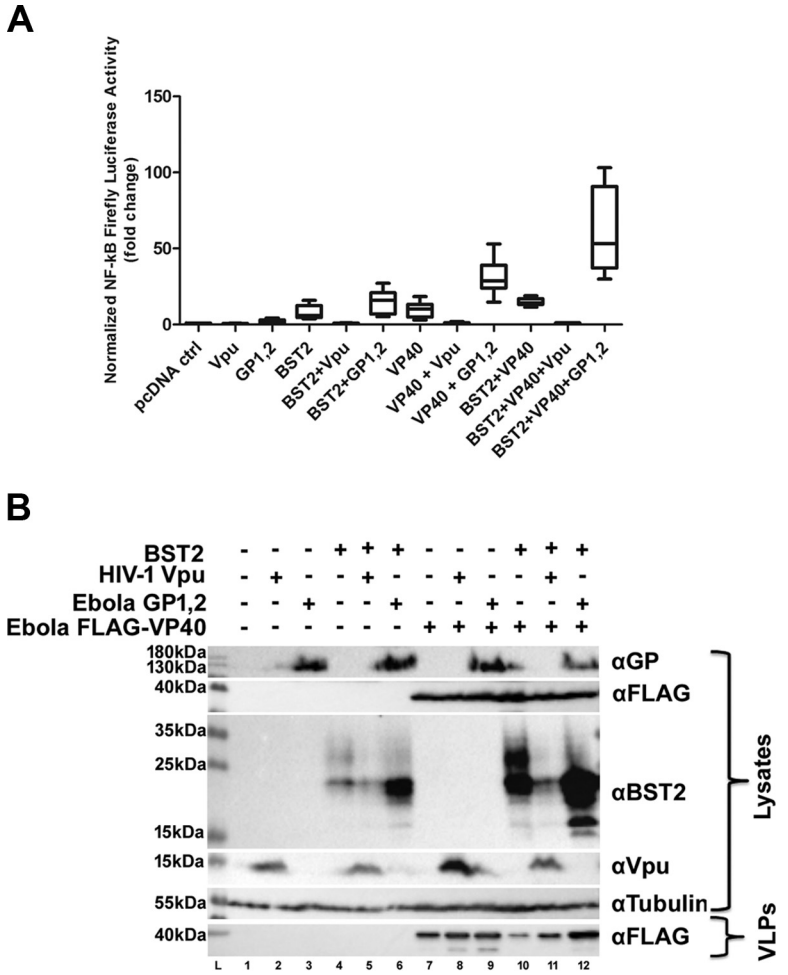

FIG 2 Ebola virus $GP_{1,2}$ and VP40 cooperate with BST2 to induce NF-κB activity in HEK293T cells that transiently express BST2. (A) Parental 293T cells were transfected with 63 ng *Renilla* luciferase plasmid and 125 ng NF-κB firefly luciferase plasmid. Wherever indicated on the graph, the cells were transfected with the following quantities of plasmids: 85 ng BST2, 300 ng VP40, 900 ng $GP_{1,2}$, and 900 ng Vpu. An empty vector, pcDNA3.1, was used to equalize the total amount of plasmids transfected in each sample. After 24 h, NF-κB luciferase activity was measured by luminometry. The data are presented as in Fig. 1A, with the pcDNA control set to 1.0. The boxes represent medians within the 25th to 75th percentile range, and the whiskers represent maximums and minimums from two independent experiments, each containing four technical replicates. Statistical analyses are presented in Tables 3 and 4. (B) Western blots of total cell lysates and isolated VLPs from one representative experiment out of two. The antibodies used for detection of the proteins are the same as those in Fig. 1B.

$GP_{1,2}$ was used in the two previous experiments and below. We observed no inhibition of NF-κB activation as a result of the expression of any of the different GPs; instead, these proteins increased NF-κB activity. We found that $rGP_{1,2}$ produced a significant increase in NF-κB activity compared to either of the Zaire ebolavirus GPs, whether expressed alone or in combination with BST2 and VP40 (Fig. 3A and Table 5). All of the GPs tested antagonized BST2 and enhanced VLP release (Fig. 3B, lane 10 versus 14 to 16). We observed increases in BST2 expression levels due to the coexpression of VP40 with the various GPs, consistent with our findings shown in Fig. 2B, in which BST2 was also expressed transiently. Overall, $GP_{1,2}$ from the two Ebola virus species cooperated with BST2 and VP40 to induce NF-κB activity, and GPs from both species effectively antagonized VLP entrapment by BST2.

BST2 and the Ebola virus proteins activate the canonical NF-κB pathway in a manner dependent on neddylation. Since we observed cooperation in the activation of NF-κB by BST2, VP40, and $GP_{1,2}$, we asked whether all these proteins use the same intracellular signaling pathway. To answer this question, we inhibited the canonical

TABLE 3 Normalized NF-κB luciferase values presented in Fig. 2A

Group	Median[a]	Min[b]	Max[c]	25th percentile	75th percentile
VP40	10.21	3.00	18.49	4.94	13.36
Vpu	0.6056	0.4146	0.97	0.51	0.81
$GP_{1,2}$	1.97	0.83	4.36	1.09	3.07
BST2	6.10	3.86	16.00	4.73	12.53
VP40 + Vpu	1.11	0.56	2.08	0.92	1.33
VP40 + $GP_{1,2}$	28.67	14.78	53.09	24.03	39.03
BST2 + VP40	14.35	11.50	18.94	13.30	17.01
BST2 + Vpu	0.781	0.5789	1.208	0.6665	1.025
BST2 + $GP_{1,2}$	15.96	5.22	27.16	6.88	20.90
BST2 + VP40 + Vpu	1.11	0.64	1.27	0.93	1.19
BST2 + VP40 + $GP_{1,2}$	53.35	29.96	103.20	37.22	90.83

[a]Control = 1.
[b]Min, minimum value.
[c]Max, maximum value.

NF-κB pathway by expressing a dominant-negative (DN), degradation-resistant IκB and by pharmacological treatment using the nedd8-activating enzyme (NAE) inhibitor MLN4924, which prevents activation of the cullin-1–RING E3 ligase complex that degrades IκB (10, 32, 33). We found that DN and wild-type (WT) IκB overexpression significantly inhibited the NF-κB activity that was induced by BST2 and the Ebola virus proteins, whether they were expressed in combination or alone (Fig. 4A and Table 6). Wild-type IκB was intended as a control, but under the conditions tested, it inhibited the induction of NF-κB activity, presumably by saturating the cullin-1-based degradative pathway. As expected, the dominant-negative, degradation-resistant IκB inhibited the induction of NF-κB activity even more effectively. Using Western blotting, we confirmed the expression of all the transfected proteins and again observed an increase in BST2 when transiently coexpressed with either $GP_{1,2}$, VP40, or both (Fig. 4B). We

TABLE 4 Statistical analysis of NF-κB luciferase signaling data presented in Fig. 2A

Group 1	Group 2	Wilcoxon rank sum	Kruskal-Wallis (control = 1)	Dunn's	Significant
pcDNA	VP40	<0.0001[d]			Yes
	Vpu	0.0122[a]			Yes
	$GP_{1,2}$	0.0051[b]			Yes
	BST2	<0.0001[d]			Yes
VP40 + Vpu	VP40		<0.0001[d]	[b]	Yes
	Vpu			[e]	No
VP40 + $GP_{1,2}$	VP40		<0.0001[d]	[b]	Yes
	$GP_{1,2}$			[c]	Yes
BST2 + VP40	VP40		0.0020[b]	[a]	Yes
	BST2			[b]	Yes
BST2 + Vpu	Vpu		<0.0001[d]	[e]	No
	BST2			[b]	Yes
BST2 + $GP_{1,2}$	$GP_{1,2}$		<0.0001[d]	[c]	Yes
	BST2			[e]	No
BST2 + VP40 + Vpu	BST2 + Vpu		<0.0001[d]	[e]	No
	BST2 + VP40			[b]	Yes
	VP40 + Vpu			[e]	No
BST2 + VP40 + $GP_{1,2}$	BST2 + $GP_{1,2}$		<0.0001[d]	[c]	Yes
	BST2 + VP40			[c]	Yes
	VP40 + $GP_{1,2}$			[e]	No

[a]$P \leq 0.05$.
[b]$P \leq 0.005$.
[c]$P \leq 0.0005$.
[d]$P < 0.0001$.
[e]Not significant.

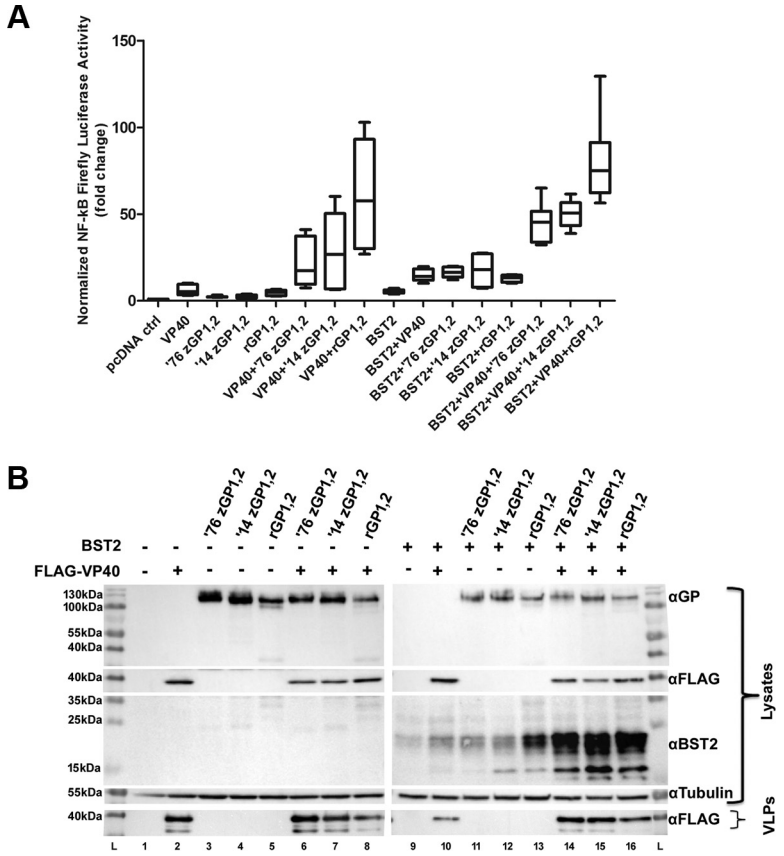

FIG 3 Ebola virus $GP_{1,2}$s from both Zaire ebolavirus and Reston ebolavirus species cooperate with VP40 and BST2 for maximal NF-κB activity. (A) Parental 293T cells were transfected with the same amounts of plasmids used in Fig. 2A. After 24 h, NF-κB luciferase activity was measured by luminometry. The boxes represent medians within the 25th to 75th percentile range of data, and the whiskers represent maximums and minimums. Statistics corresponding to the figure are provided in Table 5. (B) Western blots of total cell lysates and isolated VLPs from one representative experiment out of two. The antibodies used for detection of the proteins are the same as those in Fig. 1.

found that MLN4924 significantly and substantially inhibited NF-κB activity in a manner similar to the overexpression of IκB (Fig. 4C and Table 7). As a control for MLN4924 activity in HEK293T cells, we found that signaling by tumor necrosis factor alpha (TNF-α), which utilizes the canonical pathway of NF-κB activation, was suppressed by MLN4924 treatment. Thus, the data suggest a cooperative signaling activity between

TABLE 5 Statistical analyses of differences in NF-κB signaling presented in Fig. 3A

Group 1	Group 2	Wilcoxon rank sum (control = 1)	Significant
76 $zGP_{1,2}$	14 $zGP_{1,2}$	0.7984[c]	No
	$rGP_{1,2}$	0.0011[b]	Yes
VP40 + 76 $zGP_{1,2}$	VP40 + 14 $zGP_{1,2}$	0.9591[c]	No
	VP40 + $rGP_{1,2}$	0.0379[a]	Yes
BST2 + 76 $zGP_{1,2}$	BST2 + 14 $zGP_{1,2}$	0.9591[c]	No
	BST2 + $rGP_{1,2}$	0.0379[a]	Yes
BST2 + VP40 + 76 $zGP_{1,2}$	BST2 + VP40 + 14 $zGP_{1,2}$	0.2786[c]	No
	BST2 + VP40 + $rGP_{1,2}$	0.0011[b]	Yes

[a] $P \leq 0.05$.
[b] $P \leq 0.005$.
[c] Not significant.

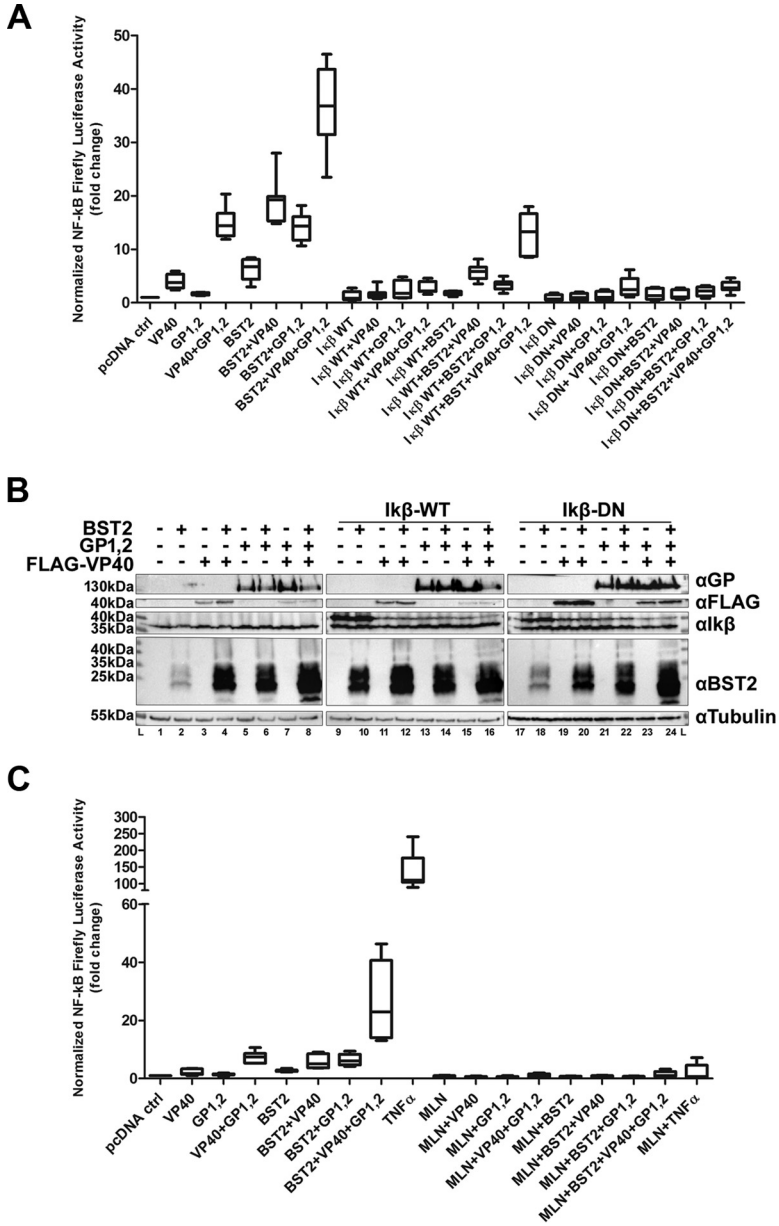

FIG 4 Ebola virus proteins signal in concert with BST2 using the canonical NF-κB pathway and neddylation. (A) HEK293T cells were transfected similarly to those in Fig. 2A, with the addition of IκB WT and DN plasmids as indicated. The box-and-whiskers graph represents two independent experiments. Statistics corresponding to the figure are shown in Table 6. (B) Western blots of total cell lysates from one experiment. Proteins were detected using the same antibodies used in Fig. 1B, in addition to mouse anti-IκB. (C) MLN4924-treated HEK293T cells compared to DMSO-treated control samples transfected similarly to those in FIG 2A. Recombinant TNF-α (40 ng/ml) diluted in 2% bovine serum albumin and 1× PBS was added for 2 h prior to harvest to the samples labeled TNF-α and MLN4924 + TNF-α. The box-and-whiskers graph represents two independent experiments. Statistics for the figure are presented in Table 7. See Materials and Methods for additional details.

the Ebola virus proteins VP40 and $GP_{1,2}$ and BST2 that merges at the canonical NF-κB activation pathway and requires neddylation.

Determinants of BST2-mediated activation of NF-κB in the context of Ebola virus protein expression. We next wanted to determine whether the maximal activation of NF-κB that we observed when BST2 was coexpressed with VP40 and $GP_{1,2}$ depended on the motifs and residues previously described as important for BST2 signaling when BST2 was expressed in isolation or in the context of retroviral assembly.

TABLE 6 Statistical analyses of differences in NF-κB signaling presented in Fig. 4A

Group 1	Group 2	Wilcoxon rank sum[d]	Significant
pcDNA	IκB-WT	0.7209[c]	No
	IκB-DN	0.2786[c]	No
VP40	VP40 + IκB-WT	**0.0019**[a]	Yes
	VP40 + IκB-DN	**0.0002**[b]	Yes
$GP_{1,2}$	$GP_{1,2}$ + IκB-WT	**1.0000**[c]	No
	$GP_{1,2}$ + IκB-DN	**0.5054**[c]	No
VP40 + $GP_{1,2}$	VP40 + $GP_{1,2}$ + IκB-WT	**0.0002**[b]	Yes
	VP40 + $GP_{1,2}$ + IκB-DN	**0.0002**[b]	
BST2	BST2 + IκB-WT	**0.0002**[b]	Yes
	BST2 + IκB-DN	**0.0002**[b]	
BST2 + VP40	BST2 + VP40 + IκB-WT	**0.0002**[b]	Yes
	BST2 + VP40 + IκB-DN	**0.0002**[b]	
BST2 + $GP_{1,2}$	BST2 + $GP_{1,2}$ + IκB-WT	**0.0002**[b]	Yes
	BST2 + $GP_{1,2}$ + IκB-DN	**0.0002**[b]	
BST2 + VP40 + $GP_{1,2}$	BST2 + VP40 + $GP_{1,2}$ + IκB-WT	**0.0002**[b]	Yes
	BST2 + VP40 + $GP_{1,2}$ + IκB-DN	**0.0002**[b]	

[a]$P \leq 0.005$.
[b]$P \leq 0.0005$.
[c]Not significant.
[d]*P* values in bold are for comparisons in which the pcDNA control was set to 1.

First, we tested the cytoplasmic tyrosine 6 and 8 alanine substitution mutants of BST2, expressed either alone or in combination with the Ebola virus proteins. As expected, we observed that BST2-Y6A and BST2-Y6,8A, but not BST2-Y8A, were significantly impaired for signaling when expressed alone. The same trend was observed when these mutants were coexpressed with the Ebola virus proteins; BST2-Y6A and -Y6,8A did not cooperate with the Ebola virus proteins to induce the high level of NF-κB activity observed with wild-type BST2 (Fig. 5A and Table 8). We confirmed by Western blotting that all the proteins were expressed (Fig. 5B). These data suggested that the cooperative activation of NF-κB by BST2 and the Ebola virus proteins occurs by a mechanism the same as or similar to what has been proposed for BST2 signaling in other settings, that is, via the cytoplasmic tyrosine 6 residue.

Next, we wanted to extend this apparent mechanistic similarity through the use of additional examples. To do this, we tested ectodomain mutants of BST2: a putative tetramerization mutant (L70D), a glycosylation mutant in which the two ectodomain asparagines that are subject to N-linked glycosylation were mutated to glutamines (N2Q), a mutant impaired for cysteine-dependent dimerization (C3A), and a mutant

TABLE 7 Statistical analyses of differences in NF-κB signaling presented in Fig. 4C

Group 1	Group 2	Wilcoxon rank sum[e]	Significant
pcDNA	pcDNA + MLN[d]	0.0530[c]	No
TNF-α	TNF-α + MLN	**0.0006**[b]	Yes
VP40	VP40 + MLN	**0.0006**[b]	Yes
$GP_{1,2}$	$GP_{1,2}$ + MLN	**0.0012**[a]	Yes
VP40 + $GP_{1,2}$	VP40 + $GP_{1,2}$ + MLN	**0.0006**[b]	Yes
BST2	BST2 + MLN	**0.0006**[b]	Yes
BST2 + VP40	BST2 + VP40 + MLN	**0.0006**[b]	Yes
BST2 + $GP_{1,2}$	BST2 + $GP_{1,2}$ + MLN	**0.0006**[b]	Yes
BST2 + VP40 + $GP_{1,2}$	BST2 + VP40 + $GP_{1,2}$ + MLN	**0.0006**[b]	Yes

[a]$P \leq 0.005$.
[b]$P \leq 0.0005$.
[c]Not significant.
[d]MLN, MLN4924.
[e]*P* values in bold are for comparisons in which the pcDNA control was set to 1.

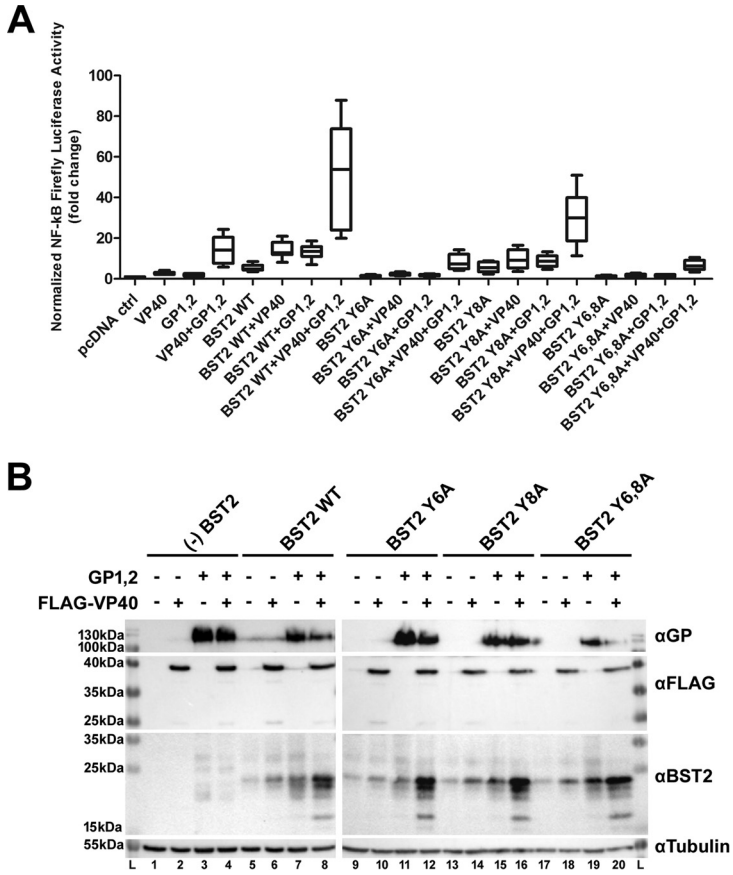

FIG 5 BST2 signaling in concert with Ebola virus proteins requires the cytoplasmic tyrosine 6 residue. (A) Parental 293T cells were transfected similarly to those in Fig. 2A. After 24 h, NF-κB luciferase activity was measured by luminometry. The box-and-whiskers graph represents two independent experiments. Statistics for the figure are presented in Table 8. (B) Western blots of total cell lysates from one representative experiment out of two. The antibodies used for detection of the proteins were the same as in Fig. 1B.

lacking the GPI anchor signal sequence (specifically an in-frame deletion of that sequence from residues 156 to 162). These mutants were expressed in HEK293T cells either alone or in combination with the Ebola virus proteins. We tested their abilities to activate NF-κB, entrap VLPs, and respond to $GP_{1,2}$-mediated counteraction of VLP entrapment (Fig. 6). Compared to wild-type BST2, we found that the BST2-L70D and -C3A mutants were statistically significantly impaired in their ability to activate NF-κB, whether expressed alone or in concert with the Ebola virus proteins (Fig. 6A and Table 9). In contrast, we did not observe a significant difference in NF-κB activation between BST2-N2Q and wild-type BST2, whether alone or with the Ebola virus proteins. Interestingly, we found a significant increase in NF-κB activation by the BST2-ΔGPI mutant compared to wild-type BST2, whether alone or with the Ebola virus proteins (Fig. 6A and Table 9). This ability of BST2-ΔGPI to activate NF-κB is consistent with our previous data regarding the phenotype of the mutant when expressed in the absence of viral proteins, but it is at odds with another study of a "ΔGPI" mutant in which a stop codon occurs before the anchor sequence; that mutant was reportedly defective for signaling (2, 4, 9). We confirmed the expression of the viral proteins and all the BST2 mutants by Western blotting, which showed the expected mobility shift of the N2Q mutant (Fig. 6B). We also measured VLP release (Fig. 6B) and found that, as expected, the C3A and ΔGPI mutants were defective for VLP entrapment. Also, we found that $GP_{1,2}$ antagonized the ability of L70D and N2Q to trap virions, since the release of VLPs was restored in cells expressing those BST2 mutants in response to $GP_{1,2}$ expression (Fig. 6B, lanes

TABLE 8 Statistical analyses of differences in NF-κB signaling presented in Fig. 5A

Group 1	Group 2	Wilcoxon rank sum[d]	Significant
pcDNA	BST2-WT	0.0002[b]	Yes
	BST2-Y6A	0.1949[c]	No
	BST2-Y8A	0.0002[b]	Yes
	BST2-Y6,8A	0.5737[c]	No
BST2-WT	BST2-Y6A	**0.0002[b]**	Yes
	BST2-Y8A	**0.8785[c]**	No
	BST2-Y6,8A	**0.0002[b]**	Yes
BST2-WT + VP40	BST2-Y6A + VP40	**0.0002[b]**	Yes
	BST2-Y8A + VP40	**0.1049[c]**	No
	BST2-Y6,8A + VP40	**0.0002[b]**	Yes
BST2-WT + $GP_{1,2}$	BST2-Y6A + $GP_{1,2}$	**0.0002[b]**	Yes
	BST2-Y8A + $GP_{1,2}$	**0.0207[a]**	Yes
	BST2-Y6,8A + $GP_{1,2}$	**0.0002[b]**	Yes
BST2-WT + VP40 + $GP_{1,2}$	BST2-Y6A + VP40 + $GP_{1,2}$	**0.0002[b]**	Yes
	BST2-Y8A + VP40 + $GP_{1,2}$	**0.2345[c]**	No
	BST2-Y6,8A + VP40 + $GP_{1,2}$	**0.0002[b]**	Yes

[a] $P \leq 0.05$.
[b] $P \leq 0.0005$.
[c] Not significant.
[d] P values in bold are for comparisons in which the pcDNA control was set to 1.

10, 12, 14, and 16 versus 2). Overall, we found that the determinants in BST2 for maximal signaling combined with the Ebola virus proteins were the same as the previously reported determinants of BST2 signaling expressed alone or in the context of retroviral expression, with the possible exception of the above-noted controversy regarding mutants of the GPI anchor sequence.

Activation of NF-κB by BST2 in concert with the Ebola virus proteins is independent of VLP entrapment. Thus far, we had observed a disconnect between BST2-mediated activation of NF-κB and VLP entrapment: VLP entrapment was antagonized by $GP_{1,2}$, but NF-κB activity was enhanced (Fig. 1 and 2). We also found that the BST2 ΔGPI mutant, which is defective for VLP entrapment, was more effective than wild-type BST2 at inducing NF-κB activity (Fig. 6A and B). Here, we asked whether the ΔGPI mutant signals using the same mechanism as wild-type BST2 with respect to the requirement for tyrosine 6 (Fig. 5A). We wanted to ensure that the ΔGPI mutant was not signaling through an aberrant mechanism, perhaps associated with its mislocalization within the cell, since it does not reach the plasma membrane (5) (Fig. 7B). Consistent with a mechanistic similarity, the Y6A mutation impaired the induction of NF-κB activity by the ΔGPI mutant (Fig. 7A and Table 10), just as it impairs the activity of wild-type BST2. Using Western blotting, we confirmed the expression of all the tested proteins (Fig. 7C). We also compared the BST2-ΔGPI/Y6A mutant to wild-type BST2, BST2-ΔGPI, and BST2-Y6A for its ability to entrap VLPs. We found that the BST2-ΔGPI/Y6A mutant was defective for VLP entrapment, similar to the ΔGPI single mutant (Fig. 7C, lanes 10 and 18). These data on BST2-ΔGPI suggest that the entrapment of VLPs was not required for the induction of maximal NF-κB activity, and they support the hypothesis that BST2-ΔGPI does not signal aberrantly, at least with respect to its dependence on tyrosine 6.

Statistical analysis confirms that BST2 cooperates with Ebola virus VP40 and $GP_{1,2}$ to induce maximal NF-κB activity. The experiments presented thus far contained eight core samples that were used repeatedly as controls during the transient expression of BST2: BST2 alone, Zaire ebolavirus $GP_{1,2}$ alone, Zaire ebolavirus VP40 alone, and all the combinations of these proteins. Since substantial variations in the fold changes occurred between the experiments, we wanted to test whether statistically significant differences between the groups held true when these conditions were compared for all of the experiments together (Fig. 8 and Tables 11 and 12). To test this,

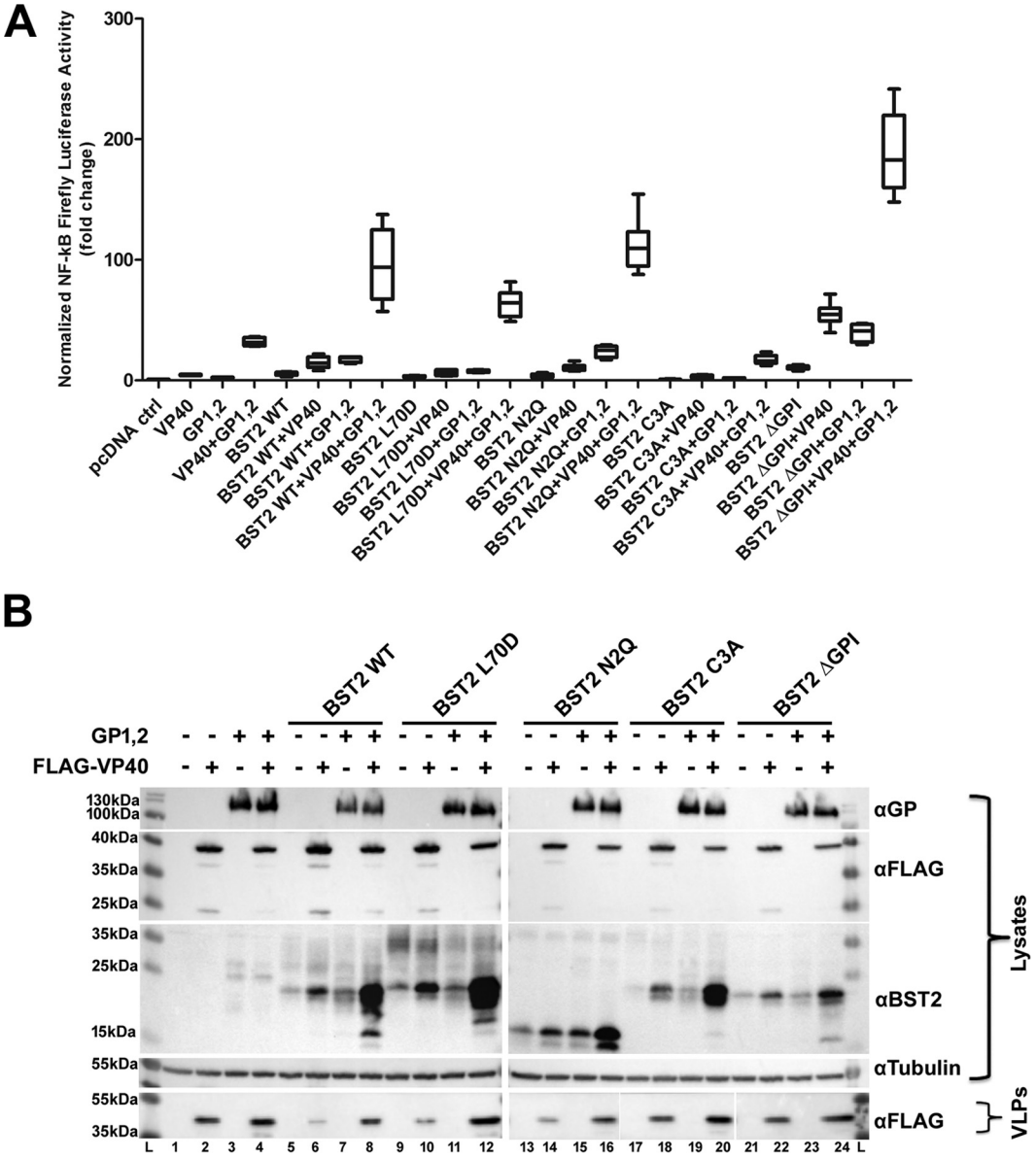

FIG 6 Optimal BST2 signaling in concert with Ebola virus proteins requires the putative L70 tetramerization residue and cysteine-dependent dimerization but not glycosylation or the GPI anchor signal sequence. (A) Parental 293T cells were transfected similarly to those in Fig. 2A with the indicated BST2 mutants at 85 ng. After 24 h, NF-κB luciferase activity was measured by luminometry. The box-and-whiskers graph represents two independent experiments. Statistics for the figure are presented in Table 9. (B) Western blots of total cell lysates and VLPs from one representative experiment out of two. The antibodies used for detection of the proteins were the same as in Fig. 1B. The VLP blots for lanes 13 through 24 are from the same gel, which was run in a different order from the lysates; therefore, the image was cut and reordered to match the order of the lanes for the lysates.

we performed statistical analysis on the 14 experiments using transient expression of BST2, each representing two independent replicates and each replicate containing two to four technical replicates, for a total of 28 independent replicates of the same groups. We used the Wilcoxon rank sum test for groups of single variables compared to background NF-κB activity; i.e., two-group comparisons pre-normalization to the background control. We found that BST2, VP40, and $GP_{1,2}$ all induced a significant increase in NF-κB activity (Table 11). We used the Kruskal-Wallis test, followed by a Dunn's multiple-comparison test, i.e., multiple-group comparisons post-normalization to the background control. The NF-κB activity induced by BST2 with $GP_{1,2}$ was significantly more than the activity induced by either protein alone (Tables 11 and 12). The NF-κB

TABLE 9 Statistical analyses of differences in NF-κB signaling presented in Fig. 6A

Group 1	Group 2	Wilcoxon rank sum[e]	Significant
pcDNA	BST2-WT	0.0002[c]	Yes
	BST2-L70D	0.0002[c]	Yes
	BST2-N2Q	0.0002[c]	Yes
	BST2-C3A	0.3282[d]	No
	BST2-ΔGPI	0.0002[c]	Yes
BST2-WT	BST2-L70D	**0.0011**[b]	Yes
	BST2-N2Q	**0.1304**[d]	No
	BST2-C3A	**0.0002**[c]	Yes
	BST2-ΔGPI	**0.0002**[c]	Yes
BST2-WT + VP40	BST2-L70D + VP40	**0.0006**[c]	Yes
	BST2-N2Q + VP40	**0.0830**[d]	No
	BST2-C3A + VP40	**0.0002**[c]	Yes
	BST2-ΔGPI + VP40	**0.0002**[c]	Yes
BST2-WT + $GP_{1,2}$	BST2-L70D + $GP_{1,2}$	**0.0286**[a]	Yes
	BST2-N2Q + $GP_{1,2}$	**0.2000**[d]	No
	BST2-C3A + $GP_{1,2}$	**0.0286**[a]	Yes
	BST2-ΔGPI + $GP_{1,2}$	**0.0286**[a]	Yes
BST2-WT + VP40 + $GP_{1,2}$	BST2-L70D + VP40 + $GP_{1,2}$	**0.0148**[a]	Yes
	BST2-N2Q + VP40 + $GP_{1,2}$	**0.3282**[d]	No
	BST2-C3A + VP40 + $GP_{1,2}$	**0.0002**[c]	Yes
	BST2-ΔGPI + VP40 + $GP_{1,2}$	**0.0002**[c]	Yes

[a] $P \leq 0.05$.
[b] $P \leq 0.005$.
[c] $P \leq 0.0005$.
[d] Not significant.
[e] *P* values in bold are for comparisons in which the pcDNA control was set to 1.

activity produced by BST2 in concert with both Ebola virus proteins (i.e., when BST2, $GP_{1,2}$, and VP40 were coexpressed) was significantly more than the activity produced by any of the three combinations of two proteins (BST2 plus VP40, BST2 plus $GP_{1,2}$, or $GP_{1,2}$ plus VP40) (Tables 11 and 12). By pooling our data sets and using rigorous statistical analyses, we supported the notion that the induction of NF-κB activity by BST2, Ebola virus $GP_{1,2}$, and Ebola virus VP40 is at least additive and that despite its ability to antagonize restricted VLP release, $GP_{1,2}$ is not an antagonist of BST2-mediated signaling.

DISCUSSION

In this study, we sought to confirm that BST2 induced NF-κB activity in response to the Ebola virus VLP-forming protein, VP40, and asked whether this signaling was reduced when BST2-mediated VLP entrapment was antagonized by Ebola virus $GP_{1,2}$. BST2 restricts the release of several families of enveloped viruses (2, 3). It also induces NF-κB activity when expressed alone or, to a greater extent, when coexpressed with the virion-forming proteins of retroviruses (4, 5).

We found that the coexpression of BST2 WT with the Ebola virus VLP-forming VP40 protein produced more NF-κB activity than either protein alone. This was observed in cells that expressed BST2 stably or transiently (Tables 1 to 4), although the effect did not reach statistical significance in the stable-expression model when analyzed by Dunn's test for multiple comparisons (Fig. 1A and Table 2). These results regarding the coexpression of BST2 with VP40 are consistent with the reported ability of BST2 to induce an increase in NF-κB activity in response to the expression of HIV-1ΔVpu and murine leukemia virus (4, 5). Consequently, the induction of NF-κB activity by BST2 in concert with VP40 could fit a model in which signaling is induced (or enhanced) by BST2 aggregation, which is presumably associated with VLP entrapment at the plasma membrane.

When we introduced the virus-encoded BST2 restriction antagonists, we found that

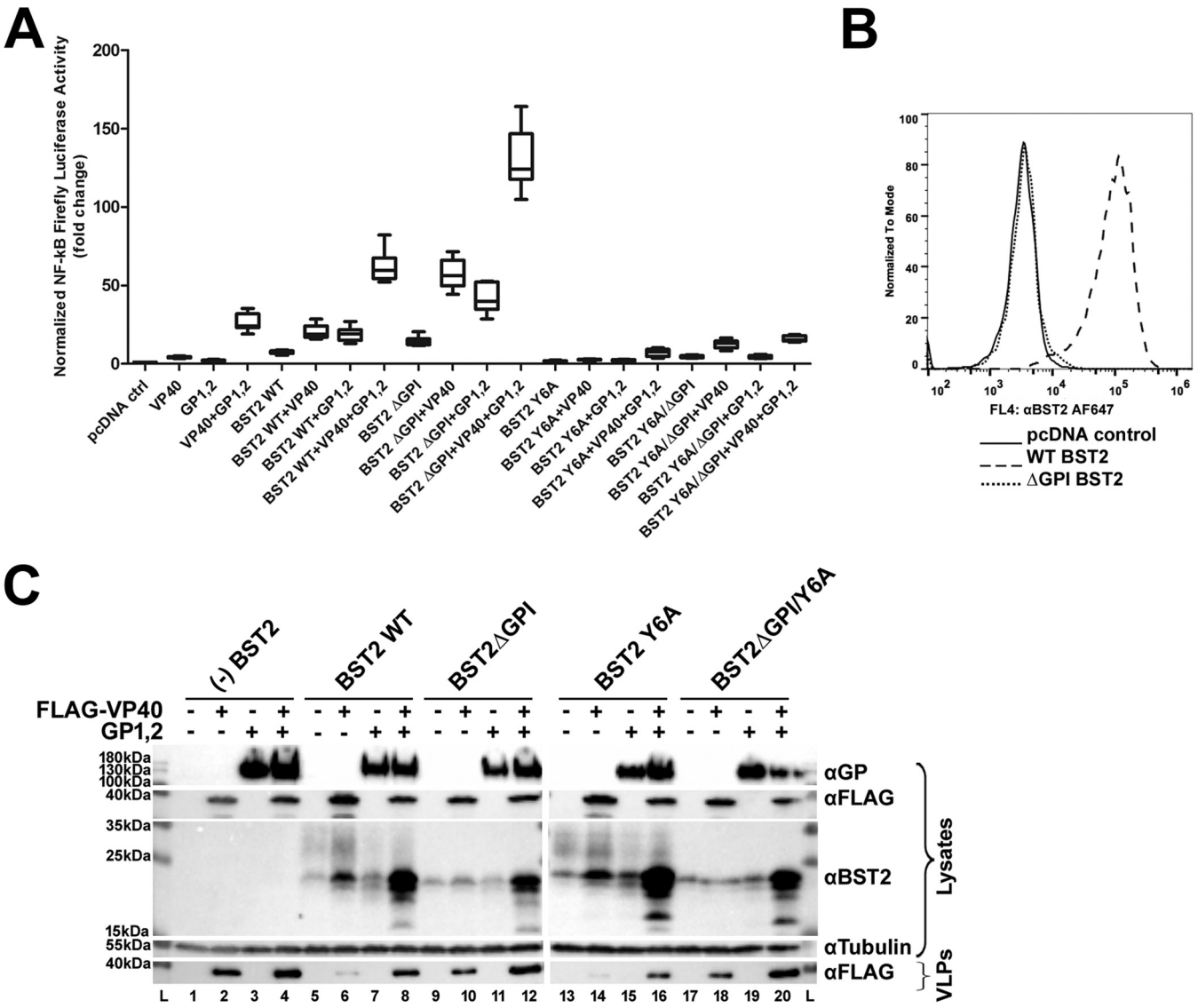

FIG 7 BST2 signaling in concert with Ebola virus proteins is independent of VLP entrapment yet dependent on the cytoplasmic tyrosine 6 of BST2. (A) HEK293T cells were transfected similarly to those in Fig. 2A with plasmids expressing the indicated BST2 mutants (85 ng). After 24 h, NF-κB luciferase activity was measured by luminometry. The box-and-whiskers graph represents two independent experiments. Statistics for the figure are in Table 10. (B) Surface BST2 WT and BST2-ΔGPI detected by flow cytometry. Green fluorescent protein (GFP) was used as a transfection control, and GFP-positive (transfected) cells are shown. (C) Western blots of total cell lysates from one representative experiment out of two. The antibodies used for detection of the proteins are the same as in Fig. 1B.

while HIV-1 Vpu inhibited NF-κB signaling, $GP_{1,2}$ did not. Although Vpu inhibits virion restriction by BST2 and thus reduces VLP entrapment at the plasma membrane, it also degrades BST2, downregulates its expression at the plasma membrane, and targets it away from virion assembly sites (13, 17, 21, 34). Any of these effects could potentially affect the activation of NF-κB. Perhaps most importantly, HIV-1 Vpu directly and generally inhibits the canonical NF-κB pathway independently of BST2 signaling; Vpu usurps the β-TrCP/cullin-1 ubiquitin ligase complex and consequently inhibits the ubiquitination and degradation of IκB (35). Thus, a primary cause of the inhibition of BST2-mediated NF-κB activation by Vpu could be its general effect on NF-κB signaling, an activity that, to our knowledge, is unique among virally encoded BST2 antagonists. This model is supported by the observation that a Vpu mutant unable to interact with BST2 nonetheless inhibits the activation of NF-κB (5). Previous reports have shown that $GP_{1,2}$ neither removes BST2 from the plasma membrane nor targets BST2 for degra-

TABLE 10 Statistical analyses of differences in NF-κB signaling presented in Fig. 7A

Group 1	Group 2	Wilcoxon rank sum[c]	Significant
pcDNA	BST2-WT	0.0002[b]	Yes
	BST2-ΔGPI	0.0002[b]	Yes
	BST2-Y6A	0.0047[a]	Yes
	BST2-Y6A/ΔGPI	0.0002[b]	Yes
BST2-WT	BST2-ΔGPI	**0.0002[b]**	Yes
	BST2-Y6A	**0.0002[b]**	Yes
	BST2-Y6A/ΔGPI	**0.0003[b]**	Yes
BST2-WT + VP40	BST2-ΔGPI + VP40	**0.0002[b]**	Yes
	BST2-Y6A + VP40	**0.0002[b]**	Yes
	BST2-Y6A/ΔGPI + VP40	**0.0006[b]**	Yes
BST2-WT + $GP_{1,2}$	BST2-ΔGPI + $GP_{1,2}$	**0.0002[b]**	Yes
	BST2-Y6A + $GP_{1,2}$	**0.0002[b]**	Yes
	BST2-Y6A/ΔGPI + $GP_{1,2}$	**0.0002[b]**	Yes
BST2-WT + VP40 + $GP_{1,2}$	BST2-ΔGPI + VP40 + $GP_{1,2}$	**0.0002[b]**	Yes
	BST2-Y6A + VP40 + $GP_{1,2}$	**0.0002[b]**	Yes
	BST2-Y6A/ΔGPI + VP40 + $GP_{1,2}$	**0.0002[b]**	Yes
BST2-ΔGPI	BST2-Y6A/ΔGPI	**0.0002[b]**	Yes
BST2-ΔGPI + VP40	BST2-Y6A/ΔGPI + VP40	**0.0002[b]**	Yes
BST2-ΔGPI + $GP_{1,2}$	BST2-Y6A/ΔGPI + $GP_{1,2}$	**0.0002[b]**	Yes
BST2-ΔGPI + VP40 + $GP_{1,2}$	BST2-Y6A/ΔGPI + VP40 + $GP_{1,2}$	**0.0002[b]**	Yes

[a] $P \leq 0.005$.
[b] $P \leq 0.0005$.
[c] *P* values in bold are for comparisons in which the pcDNA control was set to 1.

dation (25, 26); however, it does prevent the immunoprecipitation and microscopic colocalization of VP40 with BST2 (27). While these activities might be key to GP's ability to antagonize virion entrapment, they appear to have no negative influence on signaling by BST2. Instead, and paradoxically, we observed, using both stable and transient BST2 expression systems, that $GP_{1,2}$ increases NF-κB signaling when expressed together with VP40 and BST2.

Based on the above-mentioned results, we propose that, unlike the model proposed for retroviruses, VP40 VLP entrapment is not the main driving force behind the activation of NF-κB by BST2 in the setting of Ebola virus protein expression. We further

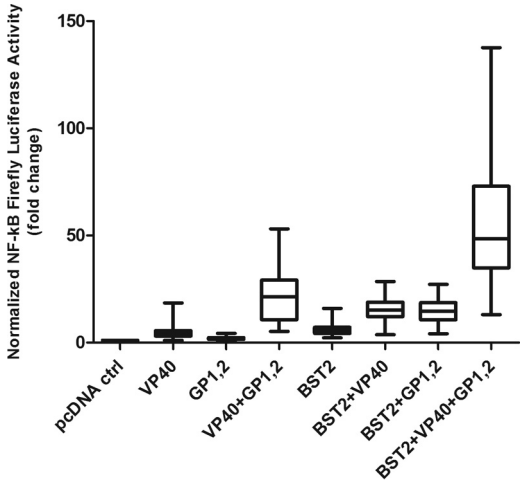

FIG 8 BST2 signaling in concert with Ebola virus VP40 and $GP_{1,2}$ as a reproducible phenotype. We combined the normalized NF-κB firefly luciferase values from the 14 independent experiments shown in Fig. 2 through 7 for the groups indicated on the box-and-whiskers graph. We used the samples expressing 1976 Zaire ebolavirus $GP_{1,2}$ for the figure. Statistical analyses are presented in Tables 11 and 12.

TABLE 11 Statistical analysis of NF-κB luciferase signaling data presented in Fig. 8

Group 1	Group2	Wilcoxon rank sum	Kruskal-Wallis (control = 1)	Dunn's	Significant
pcDNA	BST2	<0.0001[b]			Yes
	VP40	<0.0001[b]			Yes
	$GP_{1,2}$	<0.0001[b]			Yes
VP40 + GP	GP		<0.0001[b]	[a]	Yes
	VP40			[a]	Yes
BST2 + VP40	VP40		<0.0001[b]	[a]	Yes
	BST2			[a]	Yes
BST2 + GP	BST2		<0.0001[b]	[a]	Yes
	GP			[a]	Yes
BST2 + VP40 + GP	BST2 + VP40		<0.0001[b]	[a]	Yes
	VP40 + GP			[a]	Yes
	GP + BST2			[a]	Yes

[a]$P \leq 0.0005$.
[b]$P < 0.0001$.

supported this hypothesis by showing that a defect in BST2's VLP restriction function, as demonstrated by the BST2-ΔGPI mutant, did not hinder the activation of NF-κB in response to VP40 expression. Moreover, this mutant was not expressed at the cell surface, which suggests that the cooperative enhancement of NF-κB activity resulting from VP40 and BST2 coexpression did not depend on their interaction at the plasma membrane. Rather, the two proteins could be interacting within intracellular membranes.

We propose two potential explanations for how BST2, VP40, and $GP_{1,2}$ might work together to activate NF-κB. The first is simply the merging of the signaling pathways of BST2 alone and of the Ebola virus proteins alone at or before the IκB degradation step of the canonical NF-κB activation pathway. Consistent with this model, we observed that the determinants of BST2 activity in isolation were the same as the determinants of its activity in concert with the Ebola virus proteins, as demonstrated by the BST2-Y6A, BST2-Y6,8A, and C3A mutants. Expression of these BST2 mutants, along with both Ebola virus proteins, reduced the observed NF-κB activity compared to the Ebola virus proteins alone, although this reduction did not reach significance using rigorous statistical analysis. Nonetheless, these BST2 mutants might act as dominant-negative inhibitors of signaling by the Ebola virus proteins, possibly due to sequestration of shared cofactors along the signaling pathways. In this model, how VP40 and $GP_{1,2}$ induce NF-κB activity independently of BST2 requires further investigation. One mechanism that cannot be excluded by our data is VLPs containing $GP_{1,2}$ or shed forms of GP (36, 37) signaling from the extracellular space through an unknown surface receptor on HEK293T cells. Ebola virus VLPs containing $GP_{1,2}$ or extracellular shed forms of GP trigger NF-κB activation through signal transduction from the surfaces of certain cell types (37, 38). Specifically, Toll-like receptor 4 and the myeloid-specific C-type lectin

TABLE 12 Normalized NF-κB luciferase values presented in Fig. 8

Group	Median[a]	Min[b]	Max[c]	25th percentile	75th percentile
VP40	4.129	1.052	18.49	3.035	5.62
$GP_{1,2}$	1.93	0.8319	4.363	1.483	2.316
VP40 + $GP_{1,2}$	21.43	5.248	53.09	10.66	29.15
BST2	5.651	2.208	16	4.315	7.116
BST2 + VP40	15.23	3.641	28.54	12.11	18.87
BST2 + $GP_{1,2}$	14.57	4.164	27.16	10.66	18.59
BST2 + VP40 + GP	48.48	13.09	137.6	34.87	72.91

[a]Control = 1.
[b]Min, minimum value.
[c]Max, maximum value.

receptor (LSECtin) act as surface pattern recognition receptors for GP-containing VLPs and shed GP (39, 40). Extracellular signaling by VLPs formed by VP40 alone in the absence of GP seems less likely, favoring the possibility that signaling by VP40, alone or in concert with BST2, occurs by an intracellular mechanism. The second, alternative explanation is that direct intracellular interactions occur between BST2, VP40, and $GP_{1,2}$, which result in structural or conformational modifications in the proteins that enhance their ability to induce NF-κB activity. This hypothesis could be tested by defining and characterizing the signaling activities of mutants of BST2, VP40, and $GP_{1,2}$ that do not interact with each other.

How the BST2 ectodomain structure and topology contribute to the induction of NF-κB activity is not fully understood. We have previously shown and confirmed here that the putative tetramerization residue L70 is important for BST2 signaling, yet it is largely dispensable for virion entrapment (5). Given that the BST2 ectodomain tetramer forms *in vitro* under reducing conditions, whereas the extracellular environment is oxidizing, whether tetramerization *per se* is required for signaling is unclear. We confirmed that cysteines required for the dimerization of BST2 are required for signaling as well as virion entrapment (5). Dimerization has been proposed to provide signaling activity by juxtaposing two hemi-ITAM motifs in each of the BST2 cytoplasmic domains (the YXYXXV sequence). Each of these features of BST2 is required both for BST2 to signal on its own and for its signaling in concert with the Ebola virus proteins.

While the role of the GPI anchor in BST2 signaling remains elusive, our data support its dispensability. During GPI anchor addition in the endoplasmic reticulum (ER), a C-terminal hydrophobic-membrane insertion signal sequence is cleaved, and the GPI anchor is attached to a serine residue just N terminal of the cleavage site (41, 42). The ΔGPI mutant used here encodes an in-frame deletion; the C-terminal region of the precursor protein remains encoded, potentially providing a second membrane anchor despite the lack of a GPI anchor (43). This mutant is active for signaling but defective for restriction. In contrast, the BST2-ΔGPI mutant previously reported to be defective for both signaling and virion restriction (4, 9) encodes a stop codon rather than an in-frame deletion at the site of GPI anchor addition (2); it therefore lacks a hydrophobic region that could attach the C terminus to the membrane by acting as a second TM domain. We suspect that lack of the second TM domain in the stop codon mutant, rather than its inability to trap virions at the PM, explains its inability to induce NF-κB activity. In contrast, our in-frame GPI signal deletion mutant, by virtue of its alternative mode of C-terminal membrane attachment, might maintain an ectodomain topology required for signaling. Our mutant nonetheless failed to restrict virion release, which we suspect is due to its failure to reach the plasma membrane. Based on these observations and comparisons, we propose that signaling by BST2 requires a C-terminal attachment to the plasma membrane in addition to its N-terminal TM domain. Moreover, BST2 can signal whether expressed on the plasma membrane or on intracellular membranes and whether or not it is able to entrap virions. The notion that BST2 requires a membrane-anchored C terminus to signal suggests that the topology of the protein's ectodomain is important for this function. This raises the possibility that interaction with another membrane protein(s), or BST2 multimerization, is important.

What are the caveats to our study, in particular in comparison to previous studies that focused on retroviruses? One difference is that the Ebola virus VLP system utilizes the expression of just two viral proteins rather than the whole viral genomes used in the cases of HIV-1 and MLV. As a result, we report only the isolated effects of VP40 and $GP_{1,2}$ on BST2-mediated NF-κB signaling. Nonstructural proteins of Ebola virus, which are missing in our experiments, could in principle antagonize BST2 signaling. Moreover, the absolute and relative amounts of VP40 and $GP_{1,2}$ expressed here might not be the same as those that are expressed from the intact virus. These caveats could be addressed using a full Ebola virus infection system, which requires a biosafety level 4 (BSL4) facility.

Our findings regarding the activation of NF-κB were largely reproducible in two separate HEK293T cell-based settings, one in which parental cells were engineered to

express BST2 constitutively and another in which BST2 was expressed by transient transfection from a plasmid. Differences in the molecular mass patterns observed for BST2 in these two systems were nonetheless striking (compare Fig. 1B for BST2 to the Western blots in the other figures). In the stable-expression system, as expected, higher-molecular-mass species, which are likely the more highly glycosylated and mature forms of BST2, were much more evident than in the transient-expression systems, in which lower-molecular-mass, immature forms predominate. The intensities of the BST2-specific bands were essentially unchanged by the expression of Ebola virus proteins in the stable-expression system, whereas in the transient-expression system, the intensities of low-molecular-mass BST2-specific bands were increased by the expression of the Ebola virus proteins. The basis for this phenomenon is unclear, but it might explain why, although consistently observed in replicate experiments, the increase in signaling caused by BST2 when VP40 and GP were coexpressed did not reach statistical significance in the stable-expression system, whereas it did in the transient-expression system (compare Tables 1 and 11). A possible explanation for the VP40- and GP-induced increases in BST2 expression after transient transfection is that the NF-κB activity induced by the Ebola virus proteins stimulates the cytomegalovirus (CMV) promoter that drives the expression of BST2. However, the same promoter drives BST2 expression in the HEK293T cells expressing BST2 constitutively (Hu6 cells), and as noted above, the expression of BST2 was not affected by the Ebola virus proteins in that system. Given the low molecular mass of the BST2 species that accumulated after transient expression, we speculate that they might be trapped in the ER. This speculation leads to the hypothesis that signaling by BST2 can occur from ER membranes, a hypothesis consistent with the ability of the ΔGPI mutant to signal despite its lack of residence at the plasma membrane. A limitation of our use of HEK293T cells is that they are not representative of early cellular targets during Ebola virus infections, although kidney cells are late targets during infection (44, 45). Studies using macrophages or dendritic cells will be required to extend our results to cells that are targeted early during Ebola virus infection.

In summary, our data support a model of BST2-mediated NF-κB activation that does not require the entrapment of virions at the plasma membrane. Instead of acting as an antagonist of signaling, Ebola virus $GP_{1,2}$ stimulates maximal NF-κB activity when coexpressed with VP40 and BST2. GP protein from the Reston ebolavirus species, which is not pathogenic in humans, is just as effective as an antagonist of virion entrapment and as a stimulator of signaling as are GP proteins from the Zaire ebolavirus species, which is pathogenic. Despite the lack of specific pattern recognition receptors in our cell model, Ebola virus VP40 and $GP_{1,2}$ induce NF-κB activity even in the absence of BST2. Additional studies are needed to understand the interplay between these two viral proteins and BST2 in Ebola virus infection models and through the use of cells that are specific early targets of Ebola virus infection. Determining whether other viral antagonists of virion entrapment by BST2 are, like Ebola virus GP, inactive as signaling antagonists will enable conclusions about the generalizability of models derived from the study of HIV-1 and other retroviruses regarding BST2 as a virus sensor.

MATERIALS AND METHODS

Tissue culture and plasmids. HEK293T cells (obtained from Nathaniel Landau, New York University) were maintained in Dulbecco's minimum essential medium (DMEM) containing high glucose and L-glutamine (Gibco Thermo Fisher, Waltham, MA, USA) supplemented with 10% fetal bovine serum (FBS) (Gimini Bio Products, West Sacramento, CA, USA), 1% Pen/Strep (Gibco), 1× nonessential amino acids (NEAA) (Gibco), and 1× sodium pyruvate (Gibco). The pcDNA3.1-BST2 expression plasmid was described previously (5). Hu6-BST2 stable cells were created from parental HEK293T cells by cotransfection with linearized plasmids encoding BST2 (pcDNA3.1-BST2 WT) and zeocin resistance in a 10:1 ratio. Single-cell clones were selected using zeocin. BST2 expression was screened using surface staining of BST2 with a fluorescent antibody, followed by flow cytometry. A QuikChange mutagenesis kit (Stratagene) was used to create the pcDNA3.1-BST2-Y6A, -Y8A, and -Y6,8A mutants as described previously (5, 46). pcDNA-BST2-C3A encoding BST2 with cysteine residues 53, 63, and 91 replaced with alanines has been described previously (6). The L70D putative tetramerization-defective mutants, N2Q (N65Q/N92Q) glycosylation free, and the ΔGPI (Δ156-163) mutant of BST2 were described previously (5). pCAGGS-zaire$GP_{1,2}$-His/V5 and pCAGGS-FLAG-zaireVP40 were kind gifts from Paul Bates, University of Pennsylvania. Glycoprotein

open reading frames that produce proteins corresponding to the 2014 Zaire ebolavirus strain Ebola virus/*H. sapiens*-wt/SLE/2014/Makona-EM095B (accession number AIE11800.1) and the Reston ebolavirus strain Philippine 1992 (accession number U23416.1) were cloned into expression plasmid pCAGGS by standard methods. The pcDNA3.1-VpHu plasmid expressing human codon-optimized HIV-1 Vpu was a kind gift from Klaus Strebel, National Institute of Allergy and Infectious Diseases, and was described previously (47). pRC-HA-I$\kappa\beta$ WT and pRC-HA-I$\kappa\beta$ S32/36A (DN) were kind gifts from Michael Karin, University of California, San Diego, and were described previously (48). The pGL4.74 [hRluc/TK] plasmid expressed the reporter *Renilla* luciferase (Promega) under the transcriptional control of a herpes sarcoma virus thymidine kinase promoter. The pGL4.32 [luc2P/NF-κB-RE/Hygro] NF-κB firefly luciferase (Promega) plasmid expressed firefly luciferase under the transcriptional control of five copies of an NF-κB response element. The pCG-GFP plasmid was a kind gift from Jacek Skowronski, Case Western Reserve University.

Antibodies and reagents. Rabbit antisera for BST2 and HIV-1 Vpu were obtained from the NIH AIDS Reference Repository and contributed by Klaus Strebel. Alexa-Fluor 647-conjugated anti-BST2 (RS38E) and unconjugated anti-IκB mouse monoclonal antibodies were purchased from Biolegend, Inc. (San Diego, CA, USA). Anti-tubulin and anti-FLAG monoclonal mouse antibodies were purchased from Sigma-Aldrich (St. Louis, MO, USA). Rabbit serum (R12) raised against the Ebola virus-secreted GP, which shares a common N-terminal domain with full-length, membrane-bound GP and recognizes $GP_{1,2}$, was a generous gift from Paul Bates and was described previously (12). Recombinant TNF-α was purchased from Biolegend, Inc. (San Diego, CA, USA).

SDS-PAGE and Western blotting. Cells were lysed in Western blotting sample buffer (100 mM Tris, 0.79% sodium dodecyl sulfate [SDS], 19.8% glycerol, 9.9% β-mercaptoethanol, and 0.002% bromophenol blue in deionized water). Samples were run on SDS-polyacrylamide gel electrophoresis (PAGE) gels. The proteins were then transferred into polyvinylidene difluoride (PVDF) membranes (Bio-Rad) using the Trans-blot turbo transfer apparatus (Bio-Rad). Goat anti-mouse IgG or goat anti-rabbit IgG secondary antibodies conjugated to horseradish peroxidase (HRP) (Bio-Rad) were used for detection of protein signal by chemiluminescence. Blot images were captured using the ChemiDoc MP system (Bio-Rad). Raw images were converted to the TIF format using ImageLab software (Bio-Rad) and edited using Adobe Photoshop.

Measuring NF-κB activity using a luciferase reporter system. Cells were seeded in quadruplicate wells of 12-well tissue culture plates (Corning) in DMEM without antibiotics. The next day, the cells were transfected using 5 μl of Lipofectamine 2000 (Invitrogen) following the manufacturer's protocol. The amounts of DNA used for each transfection are indicated in the figure legends. For the IκB experiment (Fig. 4A), one experimental replicate used 20 ng of the IκB plasmids and the other used 40 ng IκB plasmid. For the MLN4924 experiment (Fig. 4C), one experimental replicate used 100 nM MLN4924 and the other used 500 nM MLN4924. Cells were harvested 24 hours after transfection. Two-thirds of the cells from each well were used for the Dual-Glo luciferase assay (Promega) according to the manufacturer's protocol. A SpectraMax M3 plate reader (Molecular Devices, Sunnyvale, CA, USA) was used to measure luminescence for the signaling experiments shown in Fig. 2 through 8. The Enspire multimode plate reader (PerkinElmer, Waltham, MA, USA) was used to measure luminescence for the signaling experiments shown in Fig. 1. Using both devices, firefly luciferase activity was measured and quenched first, and *Renilla* luciferase was measured subsequently. The remaining one-third of the cells from each of the wells was used for the detection of protein expression by WB.

VLP collection and detection. One day after transfection, media from two wells of a 12-well plate were combined and cleared of cellular debris by centrifugation at 300 $\times$ *g* for 6 min at 4°C. The media were stored at −80°C or immediately added to a monolayer of 200 μl of 20% sucrose (prepared in 1$\times$ PBS) (Invitrogen, Thermo Fisher, Waltham, MA, USA). VLPs were pelleted at 23,500 $\times$ *g* for 1 hour at 4°C. The supernatants were aspirated, and the pellets were resuspended in Western blot sample buffer. The pelleted VLPs were subjected to SDS-PAGE and WB.

MLN4924 treatment. The nedd8 activation inhibitor MLN4924 was purchased from Active Biochem (Maplewood, NJ, USA) and described previously (32). The lyophilized drug was dissolved in dimethyl sulfoxide (DMSO), and aliquots were stored at −80°C. HEK293T cells were seeded in quadruplicate wells and transfected as described above. Four to 6 h after transfection, fresh DMEM containing DMSO alone or MLN4924 at 100 nM (or 500 nM) final concentration was added to the wells. The cells were harvested the next day, and luciferase activity was measured as described above.

Flow cytometry. Cells were plated in single wells of a 12-well plate. Twenty-four hours later, the cells were transfected using 200 ng pCG-GFP together with either the pcDNA3.1 control plasmid, pcDNA3.1-BST2 WT, or pcDNA3.1-ΔGPI as described above. The next day, the cells were assayed for surface BST2 expression by flow cytometry using an AF647-conjugated anti-BST2 antibody. The cells were fixed in 3% paraformaldehyde (Affymetrix, Santa Clara, CA, USA) and assayed using an Accuri C6 flow cytometer (BD Biosciences, San Jose, CA, USA). The data were analyzed using FlowJo software.

Statistical analysis. In GraphPad Prism 5, we used the Wilcoxon rank sum statistical test, assuming a 95% confidence interval, for nonparametric data to determine the statistical significance of changes in NF-κB activity when comparing two groups. We used the Kruskal-Wallis test, followed by Dunn's multiple-comparison test assuming a 95% confidence interval, to compare multiple groups of NF-κB fold changes normalized to a value of 1 for the pcDNA control. The *P* values for the Dunn's test in Tables 1, 4, and 11 refer to the significance between the indicated compared groups, adjusted for the total number of comparisons made. Box-and-whiskers graphs represent median values and the range between the 25th and 75th percentile of the data from independent experiments, where the whiskers represent the maximum and minimum values of the data.

ACKNOWLEDGMENTS

We thank Ned Landau for providing the HEK293T cells. We thank Paul Bates, Klaus Strebel, Jacek Skowronski, and the NIH AIDS Reagent Program for providing antibodies and plasmids as indicated in Materials and Methods. We thank Sonia Jain and Feng He from the University of California San Diego Center for AIDS Research (UCSD CFAR) Biostatistics Core for their help with statistical analysis. We thank David Lau for the creation of the stable BST2 cell line. We thank members of the Guatelli laboratory for their assistance with the editing of the manuscript.

The work was supported in part by the James B. Pendleton Charitable Trust, the UCSD CFAR, the San Diego Fellowship to M.G.R., and NIH grants R37AI081668 to J.G. and U19AI 109945 to C.F.B.

REFERENCES

1. Blasius AL, Giurisato E, Cella M, Schreiber RD, Shaw AS, Colonna M. 2006. Bone marrow stromal cell antigen 2 is a specific marker of type I IFN-producing cells in the naive mouse, but a promiscuous cell surface antigen following IFN stimulation. J Immunol 177:3260–3265. https://doi.org/10.4049/jimmunol.177.5.3260.
2. Neil SJ, Zang T, Bieniasz PD. 2008. Tetherin inhibits retrovirus release and is antagonized by HIV-1 Vpu. Nature 451:425–430. https://doi.org/10.1038/nature06553.
3. Van Damme N, Goff D, Katsura C, Jorgenson RL, Mitchell R, Johnson MC, Stephens EB, Guatelli J. 2008. The interferon-induced protein BST-2 restricts HIV-1 release and is downregulated from the cell surface by the viral Vpu protein. Cell Host Microbe 3:245–252. https://doi.org/10.1016/j.chom.2008.03.001.
4. Galao RP, Le Tortorec A, Pickering S, Kueck T, Neil SJ. 2012. Innate sensing of HIV-1 assembly by Tetherin induces NFkappaB-dependent proinflammatory responses. Cell Host Microbe 12:633–644. https://doi.org/10.1016/j.chom.2012.10.007.
5. Tokarev A, Suarez M, Kwan W, Fitzpatrick K, Singh R, Guatelli J. 2013. Stimulation of NF-kappaB activity by the HIV restriction factor BST2. J Virol 87:2046–2057. https://doi.org/10.1128/JVI.02272-12.
6. Andrew AJ, Miyagi E, Kao S, Strebel K. 2009. The formation of cysteine-linked dimers of BST-2/tetherin is important for inhibition of HIV-1 virus release but not for sensitivity to Vpu. Retrovirology 6:80. https://doi.org/10.1186/1742-4690-6-80.
7. Kupzig S, Korolchuk V, Rollason R, Sugden A, Wilde A, Banting G. 2003. Bst-2/HM1.24 is a raft-associated apical membrane protein with an unusual topology. Traffic 4:694–709. https://doi.org/10.1034/j.1600-0854.2003.00129.x.
8. Hammonds J, Wang JJ, Yi H, Spearman P. 2010. Immunoelectron microscopic evidence for Tetherin/BST2 as the physical bridge between HIV-1 virions and the plasma membrane. PLoS Pathog 6:e1000749. https://doi.org/10.1371/journal.ppat.1000749.
9. Galao RP, Pickering S, Curnock R, Neil SJ. 2014. Retroviral retention activates a Syk-dependent HemITAM in human tetherin. Cell Host Microbe 16:291–303. https://doi.org/10.1016/j.chom.2014.08.005.
10. Tan P, Fuchs SY, Chen A, Wu K, Gomez C, Ronai Z, Pan ZQ. 1999. Recruitment of a ROC1-CUL1 ubiquitin ligase by Skp1 and HOS to catalyze the ubiquitination of I kappa B alpha. Mol Cell 3:527–533. https://doi.org/10.1016/S1097-2765(00)80481-5.
11. Winston JT, Strack P, Beer-Romero P, Chu CY, Elledge SJ, Harper JW. 1999. The SCFbeta-TRCP-ubiquitin ligase complex associates specifically with phosphorylated destruction motifs in IkappaBalpha and beta-catenin and stimulates IkappaBalpha ubiquitination in vitro. Genes Dev 13:270–283. https://doi.org/10.1101/gad.13.3.270.
12. Kaletsky RL, Francica JR, Agrawal-Gamse C, Bates P. 2009. Tetherin-mediated restriction of filovirus budding is antagonized by the Ebola glycoprotein. Proc Natl Acad Sci U S A 106:2886–2891. https://doi.org/10.1073/pnas.0811014106.
13. Hauser H, Lopez LA, Yang SJ, Oldenburg JE, Exline CM, Guatelli JC, Cannon PM. 2010. HIV-1 Vpu and HIV-2 Env counteract BST-2/tetherin by sequestration in a perinuclear compartment. Retrovirology 7:51. https://doi.org/10.1186/1742-4690-7-51.
14. Mansouri M, Viswanathan K, Douglas JL, Hines J, Gustin J, Moses AV, Fruh K. 2009. Molecular mechanism of BST2/tetherin downregulation by K5/MIR2 of Kaposi's sarcoma-associated herpesvirus. J Virol 83:9672–9681. https://doi.org/10.1128/JVI.00597-09.
15. Zhang F, Wilson SJ, Landford WC, Virgen B, Gregory D, Johnson MC, Munch J, Kirchhoff F, Bieniasz PD, Hatziioannou T. 2009. Nef proteins from simian immunodeficiency viruses are tetherin antagonists. Cell Host Microbe 6:54–67. https://doi.org/10.1016/j.chom.2009.05.008.
16. Goffinet C, Allespach I, Homann S, Tervo HM, Habermann A, Rupp D, Oberbremer L, Kern C, Tibroni N, Welsch S, Krijnse-Locker J, Banting G, Krausslich HG, Fackler OT, Keppler OT. 2009. HIV-1 antagonism of CD317 is species specific and involves Vpu-mediated proteasomal degradation of the restriction factor. Cell Host Microbe 5:285–297. https://doi.org/10.1016/j.chom.2009.01.009.
17. Iwabu Y, Fujita H, Kinomoto M, Kaneko K, Ishizaka Y, Tanaka Y, Sata T, Tokunaga K. 2009. HIV-1 accessory protein Vpu internalizes cell-surface BST-2/tetherin through transmembrane interactions leading to lysosomes. J Biol Chem 284:35060–35072. https://doi.org/10.1074/jbc.M109.058305.
18. Mangeat B, Gers-Huber G, Lehmann M, Zufferey M, Luban J, Piguet V. 2009. HIV-1 Vpu neutralizes the antiviral factor Tetherin/BST-2 by binding it and directing its beta-TrCP2-dependent degradation. PLoS Pathog 5:e1000574. https://doi.org/10.1371/journal.ppat.1000574.
19. Andrew A, Strebel K. 2010. HIV-1 Vpu targets cell surface markers CD4 and BST-2 through distinct mechanisms. Mol Aspects Med 31:407–417. https://doi.org/10.1016/j.mam.2010.08.002.
20. Dube M, Paquay C, Roy BB, Bego MG, Mercier J, Cohen EA. 2011. HIV-1 Vpu antagonizes BST-2 by interfering mainly with the trafficking of newly synthesized BST-2 to the cell surface. Traffic 12:1714–1729. https://doi.org/10.1111/j.1600-0854.2011.01277.x.
21. Lewinski MK, Jafari M, Zhang H, Opella SJ, Guatelli J. 2015. Membrane anchoring by a C-terminal tryptophan enables HIV-1 Vpu to displace bone marrow stromal antigen 2 (BST2) from sites of viral assembly. J Biol Chem 290:10919–10933. https://doi.org/10.1074/jbc.M114.630095.
22. Kuhl A, Banning C, Marzi A, Votteler J, Steffen I, Bertram S, Glowacka I, Konrad A, Sturzl M, Guo JT, Schubert U, Feldmann H, Behrens G, Schindler M, Pohlmann S. 2011. The Ebola virus glycoprotein and HIV-1 Vpu employ different strategies to counteract the antiviral factor tetherin. J Infect Dis 204(Suppl 3):S850–S860. https://doi.org/10.1093/infdis/jir378.
23. Gnirss K, Fiedler M, Kramer-Kuhl A, Bolduan S, Mittler E, Becker S, Schindler M, Pohlmann S. 2014. Analysis of determinants in filovirus glycoproteins required for tetherin antagonism. Viruses 6:1654–1671. https://doi.org/10.3390/v6041654.
24. Vande Burgt NH, Kaletsky RL, Bates P. 2015. Requirements within the Ebola viral glycoprotein for tetherin antagonism. Viruses 7:5587–5602. https://doi.org/10.3390/v7102888.
25. Lopez LA, Yang SJ, Hauser H, Exline CM, Haworth KG, Oldenburg J, Cannon PM. 2010. Ebola virus glycoprotein counteracts BST-2/Tetherin restriction in a sequence-independent manner that does not require tetherin surface removal. J Virol 84:7243–7255. https://doi.org/10.1128/JVI.02636-09.
26. Lopez LA, Yang SJ, Exline CM, Rengarajan S, Haworth KG, Cannon PM. 2012. Anti-tetherin activities of HIV-1 Vpu and Ebola virus glycoprotein do not involve removal of tetherin from lipid rafts. J Virol 86:5467–5480. https://doi.org/10.1128/JVI.06280-11.
27. Gustin JK, Bai Y, Moses AV, Douglas JL. 2015. Ebola virus glycoprotein promotes enhanced viral egress by preventing Ebola VP40 from associ-

ating with the host restriction factor BST2/Tetherin. J Infect Dis 212(Suppl 2):S181–S190. https://doi.org/10.1093/infdis/jiv125.
28. Brinkmann C, Nehlmeier I, Walendy-Gnirss K, Nehls J, Gonzalez Hernandez M, Hoffmann M, Qiu X, Takada A, Schindler M, Pohlmann S. 2016. The Tetherin antagonism of the Ebola virus glycoprotein requires an intact receptor-binding domain and can be blocked by GP1-specific antibodies. J Virol 90:11075–11086. https://doi.org/10.1128/JVI.01563-16.
29. Noda T, Sagara H, Suzuki E, Takada A, Kida H, Kawaoka Y. 2002. Ebola virus VP40 drives the formation of virus-like filamentous particles along with GP. J Virol 76:4855–4865. https://doi.org/10.1128/JVI.76.10.4855-4865.2002.
30. Licata JM, Johnson RF, Han Z, Harty RN. 2004. Contribution of ebola virus glycoprotein, nucleoprotein, and VP24 to budding of VP40 virus-like particles. J Virol 78:7344–7351. https://doi.org/10.1128/JVI.78.14.7344-7351.2004.
31. Volchkov VE, Feldmann H, Volchkova VA, Klenk HD. 1998. Processing of the Ebola virus glycoprotein by the proprotein convertase furin. Proc Natl Acad Sci U S A 95:5762–5767. https://doi.org/10.1073/pnas.95.10.5762.
32. Soucy TA, Smith PG, Milhollen MA, Berger AJ, Gavin JM, Adhikari S, Brownell JE, Burke KE, Cardin DP, Critchley S, Cullis CA, Doucette A, Garnsey JJ, Gaulin JL, Gershman RE, Lublinsky AR, McDonald A, Mizutani H, Narayanan U, Olhava EJ, Peluso S, Rezaei M, Sintchak MD, Talreja T, Thomas MP, Traore T, Vyskocil S, Weatherhead GS, Yu J, Zhang J, Dick LR, Claiborne CF, Rolfe M, Bolen JB, Langston SP. 2009. An inhibitor of NEDD8-activating enzyme as a new approach to treat cancer. Nature 458:732–736. https://doi.org/10.1038/nature07884.
33. Kroll M, Margottin F, Kohl A, Renard P, Durand H, Concordet JP, Bachelerie F, Arenzana-Seisdedos F, Benarous R. 1999. Inducible degradation of IkappaBalpha by the proteasome requires interaction with the F-box protein h-betaTrCP. J Biol Chem 274:7941–7945. https://doi.org/10.1074/jbc.274.12.7941.
34. McNatt MW, Zang T, Bieniasz PD. 2013. Vpu binds directly to tetherin and displaces it from nascent virions. PLoS Pathog 9:e1003299. https://doi.org/10.1371/journal.ppat.1003299.
35. Bour S, Perrin C, Akari H, Strebel K. 2001. The human immunodeficiency virus type 1 Vpu protein inhibits NF-kappa B activation by interfering with beta TrCP-mediated degradation of Ikappa B. J Biol Chem 276:15920–15928. https://doi.org/10.1074/jbc.M010533200.
36. Dolnik O, Volchkova V, Garten W, Carbonnelle C, Becker S, Kahnt J, Stroher U, Klenk HD, Volchkov V. 2004. Ectodomain shedding of the glycoprotein GP of Ebola virus. EMBO J 23:2175–2184. https://doi.org/10.1038/sj.emboj.7600219.
37. Escudero-Perez B, Volchkova VA, Dolnik O, Lawrence P, Volchkov VE. 2014. Shed GP of Ebola virus triggers immune activation and increased vascular permeability. PLoS Pathog 10:e1004509. https://doi.org/10.1371/journal.ppat.1004509.
38. Martinez O, Valmas C, Basler CF. 2007. Ebola virus-like particle-induced activation of NF-kappaB and Erk signaling in human dendritic cells requires the glycoprotein mucin domain. Virology 364:342–354. https://doi.org/10.1016/j.virol.2007.03.020.
39. Wahl-Jensen V, Kurz S, Feldmann F, Buehler LK, Kindrachuk J, DeFilippis V, da Silva Correia J, Fruh K, Kuhn JH, Burton DR, Feldmann H. 2011. Ebola virion attachment and entry into human macrophages profoundly effects early cellular gene expression. PLoS Negl Trop Dis 5:e1359. https://doi.org/10.1371/journal.pntd.0001359.
40. Zhao D, Han X, Zheng X, Wang H, Yang Z, Liu D, Han K, Liu J, Wang X, Yang W, Dong Q, Yang S, Xia X, Tang L, He F. 2016. The myeloid LSECtin is a DAP12-coupled receptor that is crucial for inflammatory response induced by Ebola virus glycoprotein. PLoS Pathog 12:e1005487. https://doi.org/10.1371/journal.ppat.1005487.
41. Caras IW, Weddell GN, Williams SR. 1989. Analysis of the signal for attachment of a glycophospholipid membrane anchor. J Cell Biol 108:1387–1396. https://doi.org/10.1083/jcb.108.4.1387.
42. Rosenbaum EE, Brehm KS, Vasiljevic E, Gajeski A, Colley NJ. 2012. Drosophila GPI-mannosyltransferase 2 is required for GPI anchor attachment and surface expression of chaoptin. Vis Neurosci 29:143–156. https://doi.org/10.1017/S0952523812000181.
43. Andrew AJ, Kao S, Strebel K. 2011. C-terminal hydrophobic region in human bone marrow stromal cell antigen 2 (BST-2)/tetherin protein functions as second transmembrane motif. J Biol Chem 286:39967–39981. https://doi.org/10.1074/jbc.M111.287011.
44. Falasca L, Agrati C, Petrosillo N, Di Caro A, Capobianchi MR, Ippolito G, Piacentini M. 2015. Molecular mechanisms of Ebola virus pathogenesis: focus on cell death. Cell Death Differ 22:1250–1259. https://doi.org/10.1038/cdd.2015.67.
45. Martines RB, Ng DL, Greer PW, Rollin PE, Zaki SR. 2015. Tissue and cellular tropism, pathology and pathogenesis of Ebola and Marburg viruses. J Pathol 235:153–174. https://doi.org/10.1002/path.4456.
46. Jia X, Weber E, Tokarev A, Lewinski M, Rizk M, Suarez M, Guatelli J, Xiong Y. 2014. Structural basis of HIV-1 Vpu-mediated BST2 antagonism via hijacking of the clathrin adaptor protein complex 1. eLife 3:e02362. https://doi.org/10.7554/eLife.02362.
47. Nguyen KL, llano M, Akari H, Miyagi E, Poeschla EM, Strebel K, Bour S. 2004. Codon optimization of the HIV-1 vpu and vif genes stabilizes their mRNA and allows for highly efficient Rev-independent expression. Virology 319:163–175. https://doi.org/10.1016/j.virol.2003.11.021.
48. DiDonato J, Mercurio F, Rosette C, Wu-Li J, Suyang H, Ghosh S, Karin M. 1996. Mapping of the inducible IkappaB phosphorylation sites that signal its ubiquitination and degradation. Mol Cell Biol 16:1295–1304. https://doi.org/10.1128/MCB.16.4.1295.